New Spherical-Cutoff Methods for Long-Range Forces in Macromolecular Simulation

PETER J. STEINBACH* and BERNARD R. BROOKS*

Laboratory of Structural Biology, Division of Computer Research and Technology, National Institutes of Health, Bethesda, Maryland 20892

Received 12 July 1993; accepted 10 November 1993

ABSTRACT

New atom- and group-based spherical-cutoff methods have been developed for the treatment of nonbonded interactions in molecular dynamics (MD) simulation. A new atom-based method, force switching, leaves short-range forces unaltered by adding a constant to the potential energy, switching forces smoothly to zero over a specified range. A simple improvement to group-based cutoffs is presented: Switched group-shifting shifts the group–group potential energy by a constant before being switched smoothly to zero. Also introduced are generalizations of atom-based force shifting, which adds a constant to the Coulomb force between two charges. These new approaches are compared to existing methods by evaluating the energy of a model hydrogen-bonding system consisting of two *N*-methyl acetamide molecules and by full MD simulation. Thirty-five 150 ps simulations of carboxymyoglobin (MbCO) hydrated by 350 water molecules indicate that the new methods and atom-based shifting are each able to approximate no-cutoff results when a cutoff at or beyond 12 Å is used. However, atom-based potential-energy switching and truncation unacceptably contaminate group–group electrostatic interactions. Group-based potential truncation should not be used in the presence of explicit water or other mobile electrostatic dipoles because energy is not a state function with this method, resulting in severe heating (about 4 K/ps in the simulations of hydrated MbCO). The distance-dependent dielectric ($\epsilon \propto r$) is found to alter the temperature dependence of protein dynamics, suppressing anharmonic motion at high temperatures. Force switching and force shifting are the best atom-based spherical cutoffs, whereas switched group-shifting is the preferred group-based method. To achieve realistic simulations, increasing the cutoff distance from 7.5 to 12 Å or beyond is much more important than the differences among the three best cutoff methods.

*Correspondence may be addressed to either author.

Journal of Computational Chemistry, Vol. 15, No. 7, 667–683 (1994)

CC 0192-8651/94/070667-17

Introduction

The realism of any macromolecular simulation depends critically on the treatment of long-range interactions between nonbonded atoms or groups. The core-repulsion, dispersion, and electrostatic potentials are usually turned off at a cutoff distance to reduce the number of interacting pairs and hence the time of computation. Experimental support for this approximation comes from a site-directed mutagenesis study by Matthews and co-workers.[1] They observed similar thermal stabilities for 13 mutants of T4 lysozyme, in which substitutions for mobile, highly solvent-exposed, charged residues were made to vary the net protein charge from +9 to +1 e. The authors concluded that electrostatic interactions between charged surface groups separated by more than typical hydrogen-bonding or salt-bridge distances contribute little to protein stability.

Three basic approaches have traditionally been used to cut off interaction potentials: discontinuous truncation of the potential at a cutoff distance, smooth switching of the potential to zero over an interval, and continuous shifting of the potential at all distances such that its value and derivative are zero at the cutoff. Of course, the computation time is reduced at the expense of altered dynamics. Several studies[2-9] have addressed some of the pitfalls inherent in these commonly used potentials.

In this article we introduce several new spherical-cutoff methods and evaluate the old and new methods in terms of their ability to reproduce results obtained without a cutoff. We do not consider Ewald summation, which calculates the true (no-cutoff) electrostatic interactions for an infinitely repeating system. The Ewald method imposes long-range correlations on the system that may be undesirable, and it is computationally more expensive than spherical-cutoff methods. The spherical-cutoff schemes considered here do not suffer from such correlations and are more convenient than Ewald summation for many simulation applications, such as the simulation of protein hydration.[10] Cell multipole algorithms, although especially promising for large systems, can be nearly as expensive as a no-cutoff simulation for systems of about 3500 atoms or less,[11] and we will not discuss them except to compare published cell–multipole results with those obtained here with spherical-cutoff methods.

Because the evolution of any physical system is determined by the forces of interaction, it is desirable to preserve the forces to the fullest extent possible. When a spherical cutoff is used at $r = r_{off}$, preservation of the force requires reducing the magnitude of the interaction energy at $r < r_{off}$ so that the force can be attenuated gradually; energy differences should be maintained accurately at all distances $r < r_{off}$ at the expense of absolute energies. In this article we consider several new cutoff schemes in hopes of better preserving forces between nonbonded atoms and groups. The interaction of two *N*-methyl acetamide molecules is first used as a simple model of protein–protein interactions to evaluate the methods. Twenty-four 150 ps MD simulations of carboxymyoglobin (MbCO) hydrated by 350 water molecules have been performed using a dielectric constant $\epsilon = 1$ to compare the new methods to existing potential-based modification schemes. Simulations of hydrated MbCO at nine different temperatures were also performed using $\epsilon = r$ to measure the effects of a distance-dependent dielectric on protein fluctuation. For comparison with a limiting case, one simulation was performed that ignored electrostatic interactions entirely. We begin with a survey of commonly used spherical-cutoff methods, including a strong caution regarding the distance-dependent dielectric coefficient ($\epsilon \propto r$). Next, the new methods are presented. The current MbCO simulations are then discussed. Finally, several conditions to be met by a desirable long-range potential function are proposed, and the old and the new potentials are evaluated accordingly.

Spherical-Cutoff Methods

The atom-based potential energy function employed in the CHARMM program[12] models all nonbonded interactions by a sum of effective pairwise-additive Lennard–Jones and Coulomb energies:

$$V(\underline{R}) = \sum_{i<j} w_{ij} \left[S_{LJ}(r_{ij}) \left(\frac{A_{ij}}{r_{ij}^{12}} - \frac{B_{ij}}{r_{ij}^{6}} \right) + S_C(r_{ij}) \frac{q_i q_j}{4\pi\epsilon_0 \epsilon r_{ij}} \right] \quad (1)$$

where $\underline{R}$ denotes the set of all atomic coordinates specifying the system conformation, A_{ij} and B_{ij} are constants depending on the types of atoms i and j, r_{ij} is the distance separating atoms i and j, q_i (q_j)

is the partial charge of atom i (j), ϵ is the relative dielectric constant, and ϵ_0 is the permittivity of free space. The weight w_{ij} is typically set to zero for atoms i and j connected by a bond or angle (i.e., by two bonds), and w_{ij} ranges from ≈0.4 to 1.0 for "1–4 interactions" (atoms separated by three bonds). The dimensionless functions, S_{LJ} and S_C, are used to trim the Lennard–Jones and Coulomb potentials to zero at $r_{ij} = r_{\text{off}}$. CHARMM uses the same switching function for the two interactions (i.e., $S_{LJ} \equiv S_C$ when switching) but shifts them differently. The relative dielectric constant ϵ is generally taken to be unity for simulations that include explicit solvent.

When atomic interactions are switched off on the basis of the distance r_{IJ} separating the geometric centers of groups I and J, the CHARMM potential is given by

$$V(R) = \sum_{I \le J} S(r_{IJ}) \sum_{i \in I, j \in J} w_{ij} \left[\frac{A_{ij}}{r_{ij}^{12}} - \frac{B_{ij}}{r_{ij}^{6}} + \frac{q_i q_j}{4\pi\epsilon_0 \epsilon r_{ij}} \right] \quad (2)$$

For groups large enough to have internal nonbonded interactions, the $I = J$ term sums over atoms $i < j$. Group-based methods exploit the fact that Coulomb interactions involving neutral groups decay faster than $1/r$: Charge–dipole interactions decay as $1/r^2$ and dipole–dipole interactions as $1/r^3$. Atoms are therefore clustered into neutral groups as much as possible, and group-based methods then calculate either all or none of the atomic interactions between any two groups. CHARMM divides each protein residue into several groups; water molecules consist of a single electrostatic group. Group-based methods are less readily vectorized than atom-based methods because they involve nested loops over atoms and groups [eq. (2)] rather than a single long loop over atoms [eq. (1)].

The strengths and weaknesses of the old and new spherical-cutoff methods can be demonstrated with a few simple test cases. Figure 1 examines the Coulomb interaction (with $\epsilon = 1$) of two unit charges of opposite sign as approximated by each of the cutoff methods discussed in this article.

Figure 2 shows our model system for interactions among neutral groups in proteins. The interaction of two rigid N-methyl acetamide molecules in the xy-plane was calculated using a standard parameter set[13] while translating one of the molecules along the intermolecular hydrogen bond (x-axis). Artificial features appear in the energy sur-

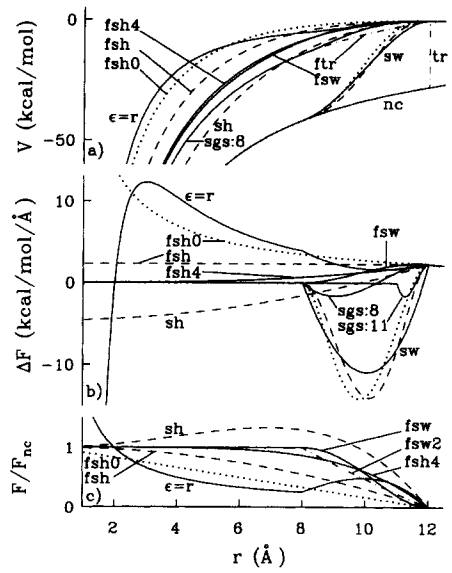

FIGURE 1. The electrostatic interaction of two unit charges of opposite sign, as approximated by different cutoff methods using $r_{\text{on}} = 8$ Å and $r_{\text{off}} = 12$ Å. The potential energy (a), the deviation from the no-cutoff constant-dielectric force, $F - F_{\text{nc}}$ (b), and the ratio of the modified force to the no-cutoff constant-dielectric force (c) are plotted. nc = no cutoff, tr = truncation, ftr = force truncation, sw = switch (solid = CHARMM,[12] dash = IMPACT,[6] dot = SPASMS[9]), sh = shift, fsh = force shift, fsh0 = generalized force shift [eq. (15)] with $\beta = 0$, fsh4 = generalized force shift [eq. (15)] with $\beta = 4$, fsw, fsw2 = atom-based force switches [eqs. (7) and (10), respectively], sgs = switched group-shift (shown for both $r_{\text{on}} = 8$ and 11 Å). Also shown is the distance-dependent dielectric potential ($\epsilon = r$), switched from 8 to 12 Å.

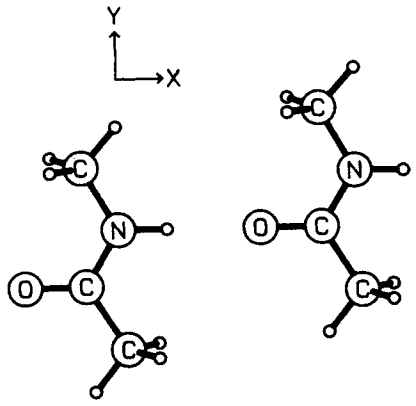

FIGURE 2. Model system for neutral-group interactions in proteins. Small circles represent hydrogen atoms. The N-methyl acetamide molecule on the right was translated along the x-axis to compare the cutoff methods (see Figs. 3, 4, and 5).

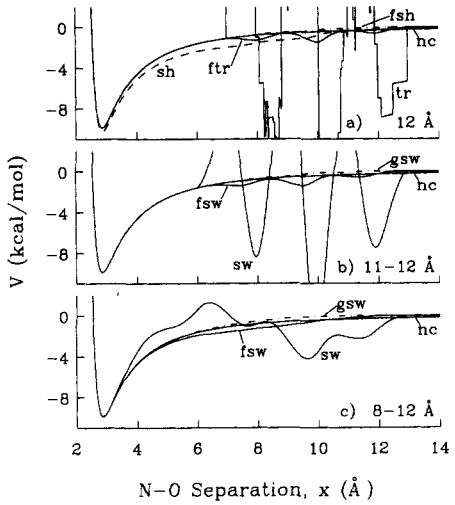

FIGURE 3. Interaction energy of two rigid *N*-methyl acetamide molecules displaced along the intermolecular hydrogen bond, approximated by different cutoff methods with r_{off} = 12 Å. Nonswitching methods (a) and methods employing a 1 Å (b) and 4 Å (c) switching region are shown. Abbreviations are as in Figure 1 with gsw = group-based switch. (Here, only CHARMM's switching function is represented as sw.) The no-cutoff (nc) energy is plotted in each panel as a solid line.

face (Fig. 3) upon separation of these neutral molecules as attractive and repulsive electrostatic interactions are alternately turned off. Note the improvement in the energy surface achieved with

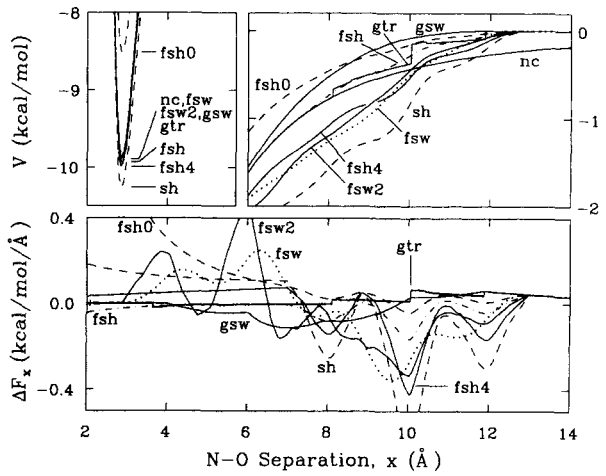

FIGURE 4. *N*-methyl acetamide interaction along the intermolecular hydrogen bond. The potential energy near the minimum (top left) and at long range (top right) are shown as well as the error in the intermolecular force along the *x*-axis (bottom), r_{off} = 12 Å. Abbreviations are as in Figures 1 and 3. For the fsw, fsw2, and gsw methods, r_{on} = 8 Å.

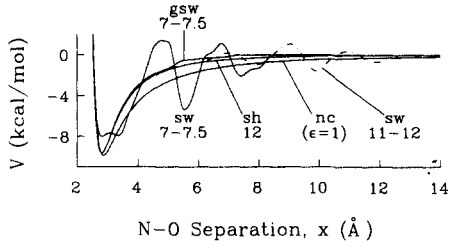

FIGURE 5. *N*-methyl acetamide interaction along the intermolecular hydrogen bond, approximated by the distance-dependent dielectric ($\epsilon = r$) with various cutoff methods. Abbreviations are as in Figures 1 and 3. The no-cutoff results with ϵ = 1 (nc) is shown for comparison. On this scale, the 12 Å shifted potential with $\epsilon = r$ is indistinguishable from the no-cutoff potential with $\epsilon = r$.

potential- and force-switching methods upon increasing the width of the switching region from 1 Å (Fig. 3b) to 4 Å (Fig. 3c). The same interaction is used in Figure 4 to compare more closely the most promising methods. The effects of using $\epsilon = r$ with some traditional cutoff methods are shown in Figure 5. Figures 1, 3, 4, and 5 each focus attention on a single degree of freedom in a simple system. In many cases, these simple interactions identify the origin of phenomena simulated in larger systems, and the figures form the basis for much of the following discussion of commonly used cutoff methods and new approaches.

COMMONLY USED METHODS

Truncation

The simplest way to exclude interactions between distant atoms is discontinuously to truncate interatomic forces at a finite distance. The truncated potential (tr) corresponds to

$$S(r) = \begin{cases} 1, & r < r_{off} \\ 0, & r \geq r_{off} \end{cases} \qquad (3)$$

where r replaces r_{ij} for simplicity. The force-truncation (ftr) potential differs from the truncated potential by a constant energy offset, yielding a continuous energy at r_{off} (Fig. 1a). Both of these atom-based truncation methods produce a force identical to the no-cutoff force at $r < r_{off}$ with a discontinuous jump to zero at r_{off}. Between any two consecutive energy discontinuities seen in Figure 3a, the slope of the truncated (tr) interaction energy is equal to that of the force-truncated (ftr) curve. Because it is the forces that propagate an MD tra-

jectory, potential and force truncation yield identical dynamics even though the corresponding energies differ significantly. The two truncation schemes will produce different Monte Carlo (MC) results with potential truncation drastically overpopulating the artificial minima. Monte Carlo simulations of Cl^- in water using group-based potential truncation have resulted in an artificial accumulation of water molecules in the Cl—O radial distribution function near the cutoff distance.[14] The minimum energy of *N*-methyl acetamide interaction (Fig. 3a) as calculated with the truncated potential is −22.9 kcal/mol at 10.22 Å, far from the true minimum of −9.9 kcal/mol at 2.85 Å. The jagged energy surface obtained with potential truncation also complicates energy minimization, where it is typically assumed that a first-order Taylor expansion of the energy is justified.

Of course, energy is not conserved if there are discontinuities in the force. When simulating with atom-based truncation, the system's total energy changes as an atom moves back and forth across the force discontinuity, $\underset{\sim}{F_d}$, at $r = r_{off}$. When moving from the inside to the outside of the interaction sphere, the change in kinetic energy of the atom is $\Delta KE = \underset{\sim}{F_d} \cdot \underset{\sim}{\Delta r} = \underset{\sim}{F_d} \cdot \underset{\sim}{v}\Delta t$, but $\Delta KE = 0$ as the atom returns across the cutoff boundary from the outside. This energy change can be reduced acceptably by decreasing the time step, Δt, used to integrate the equations of motion. Atom-based truncation with a 1-fs time step has acceptably conserved energy in simulations of dehydrated protein.[5]

In addition to the heating just described, group-based truncation (gtr) suffers from a drift in total energy that is independent of the integration time step because energy is not a state function with this method. Even in the limit of an infinitesimal time step, gtr fails to conserve energy as polar groups rotate near the cutoff.[15,16] Consider an electrostatic dipole (e.g., a water molecule) initially pointing in the $-x$-direction centered at $x = r > r_{off}$ in the field of a positive charge fixed at the origin. No work is required to move the dipole along the x-axis to $x = r_{off}$. An infinitesimal amount of work, $+dw$, is required to push the dipole just inside the cutoff. A relatively large amount of negative work, $-dW$, rotates the dipole 180°, and $+dw$ pulls the dipole outside the cutoff. Once outside the interaction sphere, no additional work is required to translate the dipole to $x = r$ and rotate it by 180°, restoring it to its initial state. Thus, the system gains kinetic energy as it traverses this path in phase space; it will "roll downhill" and heat up continually. This heat, which is independent of the integration time step, must be removed unphysically from the simulation by strongly coupling the motion to a heat bath.[17]

Although truncation effects have been discussed extensively, this distinction between group-based and atom-based truncation still needs to be stressed. The simulation of a polyalanine α helix employing group-based truncation has suffered from continuous heating.[18] Schreiber and Steinhauser have also reported simulations of a solvated helix that employed group-based truncation, observing that peptide stability did not improve continually upon increasing the cutoff distance.[7] They found that a solvated helix was stable when simulated with group-based truncation at 10 Å and when simulated with Ewald summation but was unstable when simulated with group-based truncation at either 6 or at 14 Å. They argued that this oscillatory dependence of stability on the cutoff distance may result from the oscillation in the sign of the charge density extending radially from a solute atom in water. However, the hydration water of proteins is not strongly perturbed from bulk water beyond the first hydration layer[19] and is therefore unlikely to have significant structure at distances greater than 6 Å from the helix. The observed anomalous dependence of stability on cutoff distance may have been caused, in part, by the unphysical velocity rescaling required to suppress the continual heating incurred by group-based truncation.

Energy conservation has been reported for simulations of liquid water using a group-based truncation scheme with a "jump correction" applied to the atomic velocities to account for the Dirac delta force at the cutoff.[20] This approach can be viewed as group-based potential switching, using a switching region with a width approaching zero and an effective integration time step sufficiently short to conserve energy. Although this treatment is mathematically correct, the unphysically large forces that act very briefly at the cutoff resulted in a diffusion coefficient for water that was very sensitive to the cutoff distance.

As reflected by the lower velocity-scaling factors required, group-based truncation (without the jump correction) has resulted in greater heating than atom-based truncation.[5] When $r_{off} < 9$ Å, truncating by groups has overestimated atomic fluctuation more than has atom-based truncation. The heating due to dipolar reorientation inherent in

group-based truncation causes potential truncation to be less realistic when based on groups than on atoms. By contrast, both group- and atom-based potential switching conserve energy, and for a given switching region, potential-switching simulations are more realistic when based on groups than on atoms.

Switch

The switching function applied to both the atom- and group-based CHARMM potentials is given by

$$S(r) = \begin{cases} 1, & r \le r_{on} \\ \dfrac{(r_{off}^2 - r^2)^2(r_{off}^2 + 2r^2 - 3r_{on}^2)}{(r_{off}^2 - r_{on}^2)^3}, & r_{on} < r \le r_{off} \end{cases} \quad (4)$$

This cubic function of r^2 satisfies $S(r_{on}) = 1$, $S(r_{off}) = 0$, $dS/dr(r_{on}) = 0$, and $dS/dr(r_{off}) = 0$, yielding a continuous potential energy and force. Slightly different switching functions have been used by Levy and co-workers[6] in the program IMPACT and by Kollman and co-workers[9] in the program SPASMS. At the midpoint of the switching region, these functions are steeper than the one used in CHARMM to obtain a continuous second derivative of the potential energy at r_{on} and r_{off}. However, the larger slopes correspond to larger unphysical forces at the midpoint of the switching region (Fig. 1b) and undermine any purported benefit of a continuous Hessian.

Compared to no-cutoff simulations in which all long-range interactions are included, simulations of MbCO dynamics that switch off the interatomic potentials over distances shorter than 4 Å have been shown to reduce protein motion artificially, both in terms of the root mean square deviation (rmsd) from the X-ray structure and the variance in atomic position $\langle(\Delta r)^2\rangle$.[5] Inhibited motion caused by a narrow switching region has also been reported by Smith and Pettitt in MD simulations of a Zwitterionic pentapeptide in aqueous and saline solutions.[21] These simulations employed a 1-Å switching region and exhibited less peptide flexibility, dipole fluctuation, and ionic diffusion than did simulations employing Ewald summation.

Levy and co-workers have pointed out that a narrow switching region from 7.5 to 8.0 Å acceptably conserves energy over the course of a very short 3-ps simulation of α-helical decaglycine.[6] Although it is clearly a desirable feature of any MD simulation, energy conservation is by no means sufficient to guarantee realistic dynamics. Among the differentiable forms shown in Figure 3, the switching function is consistently the worst approximation to the no-cutoff energy surface because of the very large forces imposed in the switching region. In fact, the IMPACT switching function with $r_{on} = 7.5$ Å and $r_{off} = 8.0$ Å, applied to the $t = 0$ structure of hydrated MbCO used in simulations, produces an rms error in the Coulomb force acting on each atom of 70.18 kcal/mol/Å, whereas the rms error incurred by completely ignoring electrostatics is only 12.18 kcal/mol/Å. The oscillations added to the no-cutoff surface worsen as the switching region narrows and the artificial forces increase. During simulation, the system gets trapped in the unrealistic minima, reducing atomic fluctuation.[5] The wild oscillations inherent in the switched potential are only partially reduced from those shown in Figure 3 when a distance-dependent dielectric constant is used (Fig. 5), and any macromolecular simulation that reproduces experimental data using a narrow switching region[22,23] must be interpreted very cautiously.

Switching the potential based on group–group separation approximates the no-cutoff *N*-methyl acetamide interaction energy very well (Fig. 3b). However, group-based switching suffers exactly the same fate as atom-based switching when modeling interactions between two ions or charged groups (Fig. 1b). These interactions must be addressed in realistic simulations of DNA, lipid bilayers, or any system containing a significant number of charged groups. An improved group-based method, switched group-shifting, is introduced below.

Shift and Force Shift

To avoid sudden changes in the force when using a spherical cutoff, the potential energy must be altered gradually over a long distance. A shifted potential commonly used in CHARMM for modifying electrostatics is given by

$$S(r) = (1 - (r/r_{off})^2)^2, \qquad r \le r_{off} \quad (5)$$

Historically, this potential (sh) arose from the frequent simulation of macromolecules in vacuum using a distance-dependent dielectric coefficient (rdie), $\epsilon = r$. The shifted potential monotonically attenuates the rdie force: $F/F_{nc}^{rdie} = 1 - (r/r_{off})^4$, closely approximating the no-cutoff rdie potential

when r_{off} = 12 Å (Fig. 5). When applied to the constant-dielectric force, the shifting function first increases the magnitude of the force before trimming it to zero (Fig. 1c).

Coulomb interactions have also been modified using[2,24]

$$S(r) = (1 - r/r_{off})^2, \qquad r \leq r_{off} \qquad (6)$$

We refer to this method (denoted as MEI4 by Brooks et al.[2]) as the force-shifted (fsh) potential since the atom–atom force is offset from the true Coulomb force by a constant (Fig. 1b) at $r \leq r_{off}$. These constant forces partially cancel in group–group interactions. For a charge lying along the axis of a dipole, within the cutoff distance of both dipole atoms, the errors in the atom–atom forces along the dipole sum to zero. However, errors in the force do not sum vectorially to zero when the three atoms are not colinear.

Because the shifting (sh) and force-shifting (fsh) $S(r)$ functions modify the potential at all distances, both damage the short-range interactions of charged groups. The shifted potential overestimates the magnitudes of short-range forces, whereas the force-shifted potential underestimates them (Fig. 1c). However, the absence of large errors in the force results in much smaller undulations in the interaction energy of neutral groups than those resulting from the switched potential (Fig. 3). The shifted potential produces a deeper minimum than the no-cutoff potential governing *N*-methyl acetamide interaction. The shifted well is also broader and leads to overestimated atomic fluctuation with cutoffs distances shorter than 11 Å.[5]

Figure 4 shows clearly the success of the force-shifted potential in modeling the interaction of neutral groups. Integral equation methods have shown that the force-shifted potential reproduces more accurately the short-range structure of water than does the shifted potential.[2] Wodak and collaborators have compared the shifted and force-shifted potentials using r_{off} = 8.5 Å to Ewald summation in MD simulations of liquid water.[25] All structural and dynamic properties calculated—including the oxygen–oxygen and hydrogen–oxygen radial pair distribution functions, the mean potential energy per water molecule, and the translational diffusion coefficient—were closer to the Ewald result when the force-shifted potential was used.

To shift Lennard–Jones interactions efficiently, CHARMM adds $C_{ij}r_{ij}^6 + D_{ij}$ to the potential, where the constants C_{ij} and D_{ij} are chosen such that the potential and force are zero at $r_{ij} = r_{off}$. Unlike the shifted (sh) Coulomb force, this shifted Lennard–Jones force is damped monotonically to zero.

The Distance-Dependent Dielectric

Although they are becoming less prevalent, many simulations of macromolecules in vacuum have used a distance-dependent dielectric constant (rdie, $\epsilon \propto r$), with one of the aforementioned cutoff methods, to approximate electrostatic screening by solvent molecules. The rdie approximation arose from the desire to mimic solvation while avoiding the expensive evaluation of solvent–solvent interactions. In addition, no square root needed to be calculated for each interaction pair, and the range of electrostatic interactions was reduced, permitting a shorter cutoff distance. Of course, the electrostatic potential energy of one charge in the field of another is in fact proportional to $1/r$, not $1/r^2$. Furthermore, the distance-dependent dielectric incorrectly approximates electrostatic screening equivalently for all pairs of charges, regardless of the pair's proximity to solvent. Simulation of MbCO hydrated by 350 water molecules with a constant dielectric (cdie, ϵ = 1) has been shown to reproduce realistically the structure and dynamics of solvated MbCO on the 100-ps time scale.[10]

Proponents of the distance-dependent dielectric[9] might argue that for a simulation in vacuum, macromolecular structures determined by X-ray or neutron crystallography are better preserved by rdie than by cdie simulations. However, given the very large number of parameters input to a simulation, it is not surprising that a simulation employing one or more unphysical approximations could output a small number of average quantities in agreement with experiment. If the ultimate goal of MD simulation is to predict reliably, not reproduce, experimental results, then simulations must be built on a physically justifiable foundation. In other words, if an rdie simulation and a cdie simulation produce the same average structural and dynamic quantities, the cdie simulation will afford the best predictions of detailed behavior due to its more reasonable underpinnings. Furthermore, if polarizability is ultimately to be included in the potential function, then constant-dielectric simulations lacking polarizability must first be characterized extensively.

Although we recommend against the continued use of the distance-dependent dielectric for the

aforementioned reasons, we have performed rdie simulations at multiple temperatures to measure the sensitivity of protein dynamics to modifications to long-range interactions. To demonstrate best the consequences of the rdie potential, we have applied it with a very generous cutoff, a 12-Å shifted potential. This choice is generous because on the scale of Figure 5, the 12-Å shifted rdie potential is indistinguishable from the no-cutoff rdie potential. Compared to the cdie potential, the rdie potential shortens the hydrogen bond slightly and narrows the potential well in the *N*-methyl acetamide interaction (Fig. 5). Note that the rdie potential, used with a switching region from 7 to 7.5 Å,[22,23] fails to approximate reasonably the *N*-methyl acetamide interaction, contaminating the minimum and adding several artificial ones.

NEW APPROACHES

Force Switch

We now introduce an atom-based force-switching method (fsw) that reproduces forces identically at short range and damps them monotonically to zero in the interval from r_{on} to r_{off}. That is, the force, not the potential energy, is switched off by the multiplicative function $S(r)$. Berne and co-workers have applied switching functions to the force to separate multiple time scales for the efficient simulation of simple systems with short- and long-range forces.[26] Continuity of d^2V/dr^2 is obtained by switching any force with the switching function of eq. (4). The potential energy is obtained by integrating the switched force:

$$V(r) = \begin{cases} V_{true}(r) + \Delta V_1, & r \le r_{on} \\ -\int_{r_{off}}^{r} dr' S(r') F_{true}(r'), & r_{on} < r \le r_{off} \end{cases} \quad (7)$$

where ΔV_1 is determined by the continuity of $V(r)$ at r_{on}. Because $S(r)$ is cubic in r^2, the integrand above contains a r^{-1} term for any $V_{true}(r) = cr^{-n}$ with $n = 2$, 4, or 6. These potentials consequently require the expensive evaluation of a logarithm when determining the energy in the switching region. Generalizing the switching function of eq. (4) to a cubic in r^α can avoid the logarithm in such cases. For $n = 1$ and $\alpha = 2$ [eq. (4)],

$$\Delta V_1 = 8c((r_{on}r_{off})^2(r_{off} - r_{on}) - (r_{off}^5 - r_{on}^5)/5)/\gamma, \quad (8)$$

$$V(r) = c(A(r^{-1} - r_{off}^{-1}) + B(r_{off} - r) + C(r_{off}^3 - r^3) + D(r_{off}^5 - r^5)), \quad r_{on} < r \le r_{off} \quad (9)$$

where $A = r_{off}^4(r_{off}^2 - 3r_{on}^2)/\gamma$, $B = 6(r_{on}r_{off})^2/\gamma$, $C = -(r_{on}^2 + r_{off}^2)/\gamma$, $D = 2/(5\gamma)$, and $\gamma = (r_{off}^2 - r_{on}^2)^3$.

We have also tried damping the force more efficiently at the expense of discontinuities in d^2V/dr^2 at r_{on} and r_{off} and a slightly larger ΔV. Let

$$V(r) = \begin{cases} V_{true}(r) + \Delta V_2, & r \le r_{on} \\ k(r^{-\beta} - r_{off}^{-\beta})^2, & r_{on} < r \le r_{off} \end{cases} \quad (10)$$

Requiring that V and dV/dr be continuous yields ΔV_2 and k. The constant β is chosen such that the modified force F is less than or equal to the true force at all distances, a condition not met by switching or shifting the potential. Damping F monotonically requires that $d(F/F_{true})/dr \le 0$ at r_{on}, which leads to

$$n/\beta \le 2 + \frac{r_{on}^\beta}{r_{off}^\beta - r_{on}^\beta} \quad (11)$$

The choice of $\beta = n/2$ follows naturally from the definition of $V(r)$ in the force-switching region as parabolic in $r^{-\beta}$. When modifying the potential cr^{-n}, setting $\beta = n/2$ avoids large discontinuities in the second derivative and corresponds to

$$\Delta V_2 = \frac{-c}{(r_{on}r_{off})^\beta} \quad (12)$$

$$k = c\frac{r_{off}^\beta}{r_{off}^\beta - r_{on}^\beta} \quad (13)$$

This method of force switching (fsw2) is less expensive and is well suited to the Lennard–Jones interactions ($n = 6$, 12), which are much smaller in magnitude than the Coulomb interactions. The logarithm required by eqs. (7) and (4) for $n = 6$ is avoided, the discontinuity in the second derivative is acceptable for these weaker interactions, and the square root needed can be taken from the Coulomb evaluation.

As seen in Figure 3b, atom-based force switching (fsw) is not immune to artificial minima in the interaction energy when a narrow switching region is used. Although no artificially large long-range forces are introduced in any given atom–atom interaction by this new method, interactions of opposite sign are being switched off alternately. The minima and barriers introduced by force switching are considerably less pronounced than those caused by potential switching because the force-based method reduces the interaction energy at short range before trimming it to zero in the switching region (Fig. 1a). Use of a 4-Å force-switching

region eliminates the minima in the *N*-methyl acetamide interaction along the *x*-axis (Fig. 4), but a shallow well of depth 0.036 kcal/mol remains for motion along the z-axis.

We now consider the application of a switching function to group–group forces. Although atom-based force switching conserves energy, group-based force switching does not. Group-based force switching and group-based force truncation fail to conserve energy as dipoles rotate upon entering and exiting the interaction sphere at $r = r_{off}$, just as was shown above for group-based truncation. In addition, energy is not conserved by group-based force switching within the switching region, $r_{on} < r < r_{off}$. Consider the dipole J consisting of atoms i and j centered at r_J interacting with the group K centered at r_K. The true energy of interaction between these groups is $E_{JK} = \Sigma_{k\in K}(E_{ik} + E_{jk})$. The corresponding force acting on atom i in the x-direction is $-\partial E_{JK}/\partial x_i$ and the switched force (based on groups) is $-\partial V_{JK}/\partial x_i \equiv -\partial E_{JK}/\partial x_i\, S(r_{JK})$. The modified energy V_{JK} is conserved only if its mixed partial derivatives are equal. We have

$$\partial^2 V_{JK}/\partial x_i \partial x_j = \partial^2 E_{JK}/\partial x_i \partial x_j\, S(r_{JK}) + \partial E_{JK}/\partial x_j\, \partial S(r_{JK})/\partial x_i,$$

$$\partial^2 V_{JK}/\partial x_j \partial x_i = \partial^2 E_{JK}/\partial x_j \partial x_i\, S(r_{JK}) + \partial E_{JK}/\partial x_i\, \partial S(r_{JK})/\partial x_j$$

The first terms in these second derivatives are equal, and $\partial S(r_{JK})/\partial x_i = \partial S(r_{JK})/\partial x_j$. However, $\partial E_{JK}/\partial x_i \neq \partial E_{JK}/\partial x_j$, and therefore energy is not a state function and is not conserved by group-based force switching within the switching region.

Switched Group-Shift

To conserve energy in a group-based method while avoiding exceedingly large long-range forces, our approach is slightly different. We refer to this method as the switched group-shift potential (sgs). The energy of interaction between groups I and J is shifted by a constant before being scaled by a switching function:

$$V_{IJ}(\underline{R}) = S(r_{IJ})\left(V_{true}(\underline{R}) - \frac{Q_I Q_J}{4\pi\epsilon r_{off}}\right) \quad (14)$$

where $S(r_{IJ})$ is the switching function [eq. (4)] of the distance separating the geometric centers of the groups, and Q_I and Q_J are the total charge of groups I and J, respectively. Here, $V_{true}(\underline{R})$ is the sum of the unmodified atom–atom electrostatic and Lennard–Jones energies for the pair of groups. If either group is neutral, this method is equivalent to group-based potential switching [eq. (2)]. For two charged groups, however, the magnitude of the artificial forces introduced by $\partial S(r_{IJ})/\partial r$ is greatly reduced by the subtraction of a constant from $V_{true}(\underline{R})$ prior to switching off the potential. The improvement in the force acting between charged groups relative to group-based potential switching is evident in Figure 1b. This method is therefore preferred over group-based potential switching in the presence of charged groups or ions and is incorporated easily (with little cost) into an existing group-based potential-switching algorithm. Group–group forces are preserved identically for $r_{IJ} < r_{on}$ but are not damped monotonically to zero in the switching region as they are for atom-based force switching. However, unlike potential switching, the increased force does not worsen significantly upon changing the switching region from 8 → 12 Å to 11 → 12 Å (Fig. 1b).

Generalization of Force Shift

To trim the Coulomb force monotonically, we consider shifting electrostatics in a way comparable to the shifted Lennard–Jones potential:

$$V(r) = \frac{q_i q_j}{4\pi\epsilon_0\epsilon}(1/r + Cr^\beta + D), \qquad r \le r_{off} \quad (15)$$

The potential and force are zero at r_{off} when

$$C = \frac{1}{\beta r_{off}^{\beta+1}}, \quad (16)$$

$$D = -\frac{\beta + 1}{\beta r_{off}} \quad (17)$$

The force is monotonically turned off at a rate determined by β (Fig. 1c): $F/F_{nc} = 1 - (r/r_{off})^{\beta+1}$. Note that the force-shifted potential (fsh) corresponds to $\beta = 1$. In the limit $\beta \to 0$ (fsh0), the ratio of the modified force to the true force is a linear ramp from 1 to 0. As β is increased, the force is improved at short range and turned off more steeply at long range, approaching a step function (force truncation) as $\beta \to \infty$. Consequently, the discontinuity in the potential energy's second derivative at r_{off} increases with β. However, for $\beta \le 6$, the discontinuity remains smaller than for the shifted potential

without the artificially enhanced atom–atom forces that arise from the shifted potential (Fig. 1c).

Simulation of MbCO

Based on Figure 3 and on previous studies,[5,21] MD simulations were not performed using atom-based switching, truncation, or force truncation. These methods introduce unacceptably deep minima in the interaction energy of neutral groups.

An all-atom representation of MbCO hydrated by 350 water molecules was used to evaluate the more promising cutoff methods. The TIP3P (ref. 27) three-site water model was modified slightly. The water hydrogens were given a small van der Waals radius, and flexibility was incorporated by omitting internal geometry constraints. Unpublished simulations indicate that these modifications yield values for the water density, heat of vaporization, and diffusion coefficient as close to the experimental values as those obtained with the original TIP3P model.

Most of the simulations and all of the subsequent analysis were performed using CHARMM on HP/Apollo workstations. Some simulations were performed using a parallel version of CHARMM[28] running on either an INTEL iPSC/860 hypercube or on a cluster of HP 730 workstations. Integration was performed with a Verlet leap-frog algorithm and a time step of 1 fs. When applied to flexible water, this integration method produces an energy drift per degree of freedom comparable to those obtained when internal water motion is constrained. The 350 water molecules were initially placed uniformly about the crystalline conformation[29] as described previously.[30] Each simulation was preceded by 1000 steps of steepest-descents energy minimization and began with a 30-ps equilibration phase during which the velocities were scaled after every ps to equilibrate the system at 300 K. The three simulations performed with r_{off} = 7.5 Å initially terminated the nonbond list at 8 Å. After 75 ps the nonbond list was extended to 9 Å to better conserve energy. These three simulations were continued to 190 ps so that the last 100 ps would be free of velocity scaling (constant particle number, volume, energy: NVE). An average structure was derived from the last 100 ps of each simulation by averaging 1000 coordinate sets translated and rotated to best fit the crystalline structure.

The energy-minimized average structure obtained from a 300-K simulation using the 12-Å shifted potential with $\epsilon = r$ was used as the starting coordinates for subsequent 150-ps simulations with the same potential at 100, 150, 175, 200, 225, 250, 275, 300, and 325 K.

The shifted (sh), force-shifted (fsh), and generalized force-shifted (fsh0, fsh4) simulations differed only in the treatment of electrostatics; Lennard–Jones interactions were shifted in the same manner. An additional simulation was performed in which electrostatic interactions were ignored completely and Lennard–Jones interactions were shifted to zero at 12 Å.

Table I lists four important quantities: the rms error in the Coulomb force acting on each atom, calculated for the initial structure of hydrated MbCO used in the simulations; the mass-weighted rms deviations of the average simulated structure from the crystalline structure and from the average no-cutoff structure; and the mass-weighted variance in atomic position. The simulation results represent averages over the final 100 ps and are tabulated for all 2536 MbCO atoms and for the 459 backbone atoms.

Figure 6a shows the temperature dependence of protein motion, as determined from cdie ($\epsilon = 1$) (ref. 30) and from rdie ($\epsilon = r$) simulations of MbCO hydrated by 350 water molecules. The variance in atomic position, averaged over all protein atoms, exhibits a glass transition near 200 K, where $\langle(\underset{\sim}{\Delta r})^2\rangle$ deviates from the linear temperature dependence expected for a harmonic solid. Despite narrowing hydrogen-bond wells (Fig. 5), the distance-depenjdent dielectric did not result in measurably reduced harmonic fluctuation (Fig. 6a); the stretching of hydrogen bonds does not have a significant effect on $\langle(\underset{\sim}{\Delta r})^2\rangle$ at low temperatures. The adverse effect of the distance-dependent dielectric on protein motion lies in its suppression of anharmonic fluctuation at higher temperatures. The rdie simulations produced a glass-transition temperature about 20 K higher than the cdie simulations. The cdie simulations have reproduced successfully both the glass-transition temperature and the anharmonic fluctuation observed by neutron scattering experiments.[30,31] The two curves plotted in Figure 6b represent the number of dihedral angles undergoing transitions, scaled equivalently for the rdie and cdie simulations to show the correlation of dihedral interconversion with anharmonic fluctuation.[10] The number of dihedral angles undergoing transitions was not dielectric dependent, nor was the time spent in the second- and third-most populated dihedral conformations, averaged over all dihedral angles. Thus, it appears that the rdie

TABLE I.
Error in the Coulomb Force, Evaluated for the t = 0 Structure of Hydrated MbCO, and Results of the Hydrated MbCO Simulations, Averaged over the Last 100 ps.

Cutoff method	r_{on} (Å)	r_{off} (Å)	rms ΔF Coulomb (kcal/mol/Å)	rmsd (Å) X-ray Protein	rmsd (Å) X-ray Backbone	rmsd (Å) No cutoff Protein	rmsd (Å) No cutoff Backbone	$\langle(\Delta r)^2\rangle$ (Å^2) Protein	$\langle(\Delta r)^2\rangle$ (Å^2) Backbone
No cutoff (nc)			0	1.52	1.13	0	0	0.55	0.30
Ignore electrostatics			12.18	2.40	1.97			2.76	1.75
CHARMM switch (sw)	11	12	31.35						
	8	12	4.43						
IMPACT switch, ref. 6	8	12	5.43						
SPASMS switch, ref. 9	8	12	5.30						
Truncation (tr)		12	1.43						
Force truncation (ftr)		12	1.43						
Force switch (fsw)	6.5	7.5	2.10	1.46	1.10	1.51	1.13	0.41	0.23
	11	12	1.08	1.42	1.11	1.34	0.90	0.48	0.28
	8	12	0.72	1.53	1.13	1.11	0.73	0.52	0.32
	6	12	0.73	1.42	1.06	1.15	0.71	0.69	0.42
Force switch (fsw2)	6.5	7.5	1.89	1.73	1.33	1.71	1.31	0.45	0.28
	11	12	0.97	1.62	1.33	1.31	1.00	0.48	0.27
Coul = fsw, LJ = fsw2	5	7.5	1.57	1.81	1.50	1.40	1.04	0.66	0.42
	8	12	0.72	1.59	1.24	1.31	0.92	0.52	0.32
	8	12	0.72	1.47	1.12	1.01	0.58	0.54	0.34
Coul = fsw, LJ = sh	8	12	0.72	1.62	1.18	1.05	0.67	0.63	0.35
	11	15	0.49	1.50	1.16	1.18	0.71	0.53	0.33
Force shift (fsh)		7.5	1.77	1.77	1.32	1.43	0.98	0.86	0.58
		12	0.90	1.66	1.36	1.35	0.99	0.54	0.32
		15	0.64	1.53	1.16	1.11	0.62	0.65	0.38
Force shift0 (fsh0)		12	2.21	1.67	1.35	1.11	0.77	0.54	0.32
Force shift4 (fsh4)		12	0.66	1.71	1.39	1.38	1.05	0.57	0.35
Shift (sh)		7.5	2.25	1.88	1.58	1.60	1.20	0.56	0.35
		12	1.22	1.57	1.30	1.25	0.90	0.47	0.29
$\epsilon = r$, shift		12	3.58	1.19	0.88	1.31	0.92	0.43	0.25
Switched group-shift (sgs)	11	12	1.23	1.73	1.42	1.64	1.29	0.49	0.29
	8	12	1.30	2.12	1.81	1.83	1.53	0.64	0.34
Group switch (gsw)	11	12	2.18	2.03	1.56	2.00	1.46	0.36	0.21
	8	12	1.45	3.20	2.63	3.29	2.66	0.41	0.25
Group truncation (gtr)		12	1.18	2.12	1.66	1.93	1.50	1.28	0.84

potential reduced conformational exploration (i.e., $\langle(\Delta r)^2\rangle$) by suppressing more collective global motions. This suppression at high temperatures may be due, in part, to the narrower hydrogen-bond wells for group–group interactions that result from the $\epsilon = r$ potential (Fig. 5).

Discussion

Recent studies by Levy and co-workers[6] and by Guenot and Kollman[9] have supported simulation protocols, specifically atom- and residue-based

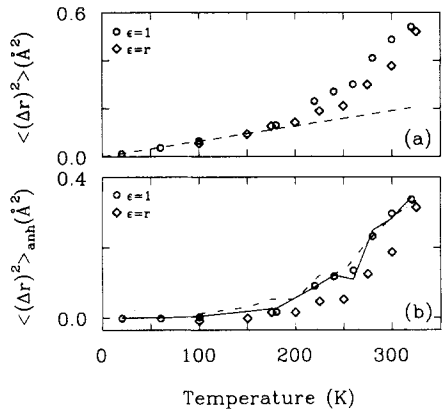

FIGURE 6. (a) Variance in atomic position $\langle(\underset{\sim}{\Delta r})^2\rangle$, averaged over all protein atoms for simulations using a 12-Å shifted potential with $\epsilon = 1$ (ref. 30) and with $\epsilon = r$. The harmonic contribution is extrapolated to high temperatures as a dashed line. (b) Anharmonic contribution obtained upon subtraction of the harmonic condition from $\langle(\underset{\sim}{\Delta r})^2\rangle$. The lines represent the number of dihedral angles undergoing transitions, scaled equally for the $\epsilon = 1$ (solid) and $\epsilon = r$ (dot-dash) simulations. The 300-K values plotted here differ from those in Table I; these were obtained from second 300-K simulations, using the final 100 ps of the simulations analyzed in Table I to generate the starting structures.

potential-switching methods, on the grounds that they conserve energy. Energy conservation is just one of many criteria to be met by a realistic cutoff scheme, and we have pointed out the serious errors introduced by switching the potential energy to zero. Guenot and Kollman speculated that of the many cutoff methods analyzed previously by Loncharich and Brooks,[5] "most of the distance-dependent and constant dielectric simulations with cutoffs ranging from 4.5 to 13.5 Å and a 1-fs time step may not conserve energy, except those that employ a switching function." This claim is clearly incorrect. Energy conservation is violated whenever forces are attenuated abruptly enough for them to change excessively during one time step. The maximum derivative of the force, $|dF/dr|$, is much larger for potential switching than for the other differentiable method considered by Loncharich and Brooks, potential shifting (see Fig. 1b). Furthermore, this maximum $|dF/dr|$ occurs at long distances for potential switching where there are the most interactions. For a given time step and cutoff distance, if potential switching conserves energy, then so will potential shifting. This energy conservation was indeed observed for the 150-ps vacuum simulations of MbCO reported by Loncharich and Brooks: For all seven rdie and for both cdie simulations at a given cutoff, the shifted potential yielded velocity-scaling factors closer to unity than did the corresponding switching-function simulations using a 1 Å region, except for rdie 13.5 Å, where equal scaling occurred. We recommend against the use of methods that fail to conserve energy, regardless of whether they are used in simulations at constant energy (NVE) or at constant temperature (NVT), but we emphasize that energy conservation alone does not ensure realistic dynamics.

Although the method conserves energy, potential switching (sw) from 11 to 12 Å results in a considerably larger rms error in the Coulomb force when applied to MbCO hydrated by 350 water molecules than does ignoring Coulomb interactions (Table I). Goddard and co-workers have argued that a 1-Å switching region results in large force errors because of the long-range interactions neglected beyond the cutoff.[32] As seen in Figure 3 and Table I, this is clearly not the case for hydrated MbCO and presumably for any other biomolecular system. The rms force error incurred by narrow switching regions results from artificially large forces introduced inside the cutoff. The neglect of long-range interactions need not result in large force errors if interactions are turned off in a reasonable fashion (Table I). The best spherical-cutoff methods produce rms errors in the Coulomb force for hydrated MbCO that, although larger, are comparable to those obtained by Goddard and coworkers with the cell multipole method (CMM) for β-alanine starburst dendrimers. Furthermore, the smooth attenuation of forces at the cutoff by spherical-cutoff methods avoids the force discontinuities that arise with the CMM at the cell boundaries, where the number of terms kept in the multipole expansion is changed abruptly. While the CMM is a promising method that deserves further characterization, the best spherical-cutoff methods yield comparable accuracy and have been evaluated more extensively.

Relatively large rms errors in the Coulomb force do not necessarily lead to severely degraded dynamics. Although the generalized force shift with $\beta = 0$ (fsh0) yielded a large rms $\underset{\sim}{\Delta F}$ of 2.21 kcal/mol/Å, it did produce realistic dynamics. The rmsd of the fsh0 structure from the X-ray structure and the fsh0 value of $\langle(\underset{\sim}{\Delta r})^2\rangle$ compare favorably with the no-cutoff results. This is because the group–group force errors obtained with fsh0 are predom-

inantly at short range (bottom panel of Fig. 4). The position of the hydrogen-bond minimum in the *N*-methyl acetamide interaction is shifted only slightly by the force error, and the well remains sufficiently deep to prevent the breaking of many hydrogen bonds.

Our previous study of protein hydration performed with the 12-Å shifted potential indicated that 350 water molecules are sufficient to hydrate MbCO on the 100-ps time scale.[10] The current study suggests that a realistic constant-dielectric simulation of MbCO dynamics requires a value of r_{off} greater than 7.5 Å. The 7.5-Å cutoff consistently resulted in drifts in the rmsd of backbone atoms to values exceeding 1.95 Å, whereas no significant drifting occurred during 150 ps of the no-cutoff or 12-Å atom-based simulations. (Although Table I suggests that the rmsd of backbone atoms in force-shifting simulations was as good with r_{off} = 7.5 Å as with r_{off} = 12 Å, the shorter cutoff distance produced a sudden structural drift in the last 25 ps of simulation.)

Of the simulations run in this study, the worst results were those obtained with group-based truncation. The system heated up continually as water molecules reoriented, requiring the velocities to be rescaled periodically. In the protocol used here, velocities were scaled if the temperature averaged over a 10-ps interval deviated by 10 K from the target temperature. During the simulation using group-based truncation, velocities needed to be scaled down every 10 ps as the temperature rose by about 40 K in each 10-ps interval. (Of the other simulations, only group-based switching from 11 to 12 Å required velocity scaling during the final 100 ps of simulation, and here only once. This was not due to lack of energy conservation but to a steady decrease in potential energy and the concurrent increase in kinetic energy during simulation. The system found a lower energy minimum with group-based switching, possibly an artificial one.) Group-based truncation is often used in simulations at constant NVT, whereas the simulations (free from velocity scaling) reported here were at constant NVE. Continuous coupling to a temperature bath (e.g., with coupling times as short as 10 fs[18]) only hides the problem inherent in group-based truncation discussed above and prohibits accurate simulation of observables sensitive to energy propagation, such as the speed of sound.

Group-based potential switching was the least realistic of the differentiable potential functions used in simulations of MbCO dynamics. This method fails because of the substantial number of charged groups in the model MbCO molecule. Of the 2536 atoms in the simulated protein, 515 are members of charged groups, resulting in a protein with net charge +1 e. When switching the potential based on groups, the rmsd from the crystalline conformation was reduced by narrowing the switching region, but atomic fluctuation was suppressed drastically from no-cutoff levels (Table I) due to the large artificial forces introduced between charged groups (Fig. 1b).

The switched group-shift method (sgs) better preserved the X-ray structure and no-cutoff fluctuation than did group-based potential switching (gsw). The MbCO dynamics obtained with sgs became more realistic as the switching region was narrowed from 8–12 Å to 11–12 Å; deviation from the crystal structure was reduced without significantly altering $\langle(\underset{\sim}{\Delta r})^2\rangle$ from the no-cutoff values (Table I). This improvement reflects the fact that the artificial forces between charged groups are enhanced significantly upon narrowing the switching region when potential switching, but not when switched group-shifting (Fig. 1b, Table I).

Although atom-based force switching may appear inferior to force shifting as judged by neutral-group interactions (Figs. 3 and 4), it is superior in handling interactions between charged groups (Fig. 1b). It consequently yields good results for simulation of MbCO (Table I) and other systems with a substantial number of charged groups. Whether r_{on} = 6, 8, or 11 Å, atom-based force switching consistently yielded rms deviations comparable to the no-cutoff simulation (Table I). Consistent with Figure 3, the atomic fluctuation predicted by the force-switching simulations using r_{off} = 12 Å increased with the width of the switching region. The 4-Å region agrees well with the no-cutoff results for both r_{off} = 12 Å and r_{off} = 15 Å.

The backbone dynamics predicted by atom-based force switching from 8 to 12 Å appear to be slightly more realistic than that predicted by either shifting or force shifting at 12 Å (Table I). Moreover, the 8–12-Å force-switching method, which employs eq. (7) for electrostatics and eq. (10) for Lennard–Jones interactions, ran at essentially the same speed as the 12-Å force-shifted potential on a scalar machine. The complexity of the evaluation in the switching region is offset by the simplicity of the evaluation at $r \leq r_{on}$ [eqs. (7) and (10)]. The shifted and force-shifted potentials, on the other hand, multiply interactions at all distances by a shifting function [eqs. (5 and 6)].

The differences in backbone dynamics among the shifted, force-shifted, and force-switched potentials are not very significant when using the relatively long cutoff distance, r_{off} = 12 Å (with r_{on} = 8 Å for fsw). Backbone deviation is only slightly reduced by force switching, and atomic fluctuation is essentially the same for these three methods. The 12-Å shifted potential has been used extensively to simulate the temperature and hydration dependence of MbCO dynamics.[10,30,33] The results of these studies—which include agreement with experiment with regard to the glass-transition temperature (about 220 K), anharmonic motion above this transition temperature, and the effects of hydration upon structure and fluctuation—are not artifacts of the shifted potential. In fact, the differences observed among the 12-Å shifted, force-shifted, and force-switched results are comparable to the difference between the force-switching results obtained from two different processors, the Apollo DN10000 and the INTEL iPSC/860 (see the two entries in Table I under "Coul = fsw, LJ = fsw2, r_{on} = 8, r_{off} = 12"). Every ps of simulated dynamics entailed 1000 force evaluations, and the dynamics diverged slowly on the two machines as tiny roundoff errors propagated. This chaoslike effect points to the general need to run several simulations, assigning initial velocities with a different random seed for each simulation. Although the improvement over the shifted and force-shifted simulations is small in the case of MbCO, the force-switching method may improve dramatically simulations of systems containing a greater percentage of charged groups.

Although the distance-dependent dielectric ($\epsilon = r$) preserved the crystalline conformation better than did any of the constant-dielectric simulations (Table I), it did so by narrowing potential wells (Fig. 5), inhibiting protein motion and shifting the glass-transition temperature (Fig. 6). The realism of MD simulations must always be evaluated in terms of both minimal structural drift and realistic fluctuation about the average structure. Preservation of the starting structure is by itself not a reliable gauge of realism. After all, the goal of MD simulations of MbCO, or of any macromolecule whose structure is known, is to reveal how the macromolecule moves and functions. Because our previous simulations of MbCO hydrated by 350 water molecules using $\epsilon = 1$ and a 12-Å shifted potential reproduced both the experimentally determined glass-transition temperature and the anharmonic motion at higher temperatures, we feel strongly that a slight increase in rmsd from the crystalline structure is well worth the realism gained in dynamics upon changing from $\epsilon = r$ to $\epsilon = 1$. Furthermore, the future in simulation does not lie with distance-dependent dielectric approximations, as solvation and polarization effects are better incorporated into the empirical energy function.

SUMMARY OF RESULTS AND OBSERVATIONS

Our evaluation of spherical-cutoff methods assumes that the best cutoff methods are those that least perturb the no-cutoff energy surface and its resultant dynamics. For the MbCO simulations, this amounted to producing a small rmsd from the X-ray structure while maintaining appropriately large motional amplitudes. The simulations of hydrated MbCO reported here prompt the following conclusions:

1. It is far more important to employ a cutoff distance of 12 Å or more than it is to worry about the differences between the best atom-based methods: force switching over a 4-Å region and force shifting.
2. Atom-based switching and truncation and group-based truncation are inferior cutoff methods and should not be used for electrostatic interactions. Atom-based switching conserves energy but produces unphysical energy minima and large force errors (Figs. 3b, 3c, 5, Table I), whereas group-based truncation heats the system continually as electrostatic dipoles reorient near the cutoff.
3. For systems containing charged groups, the switched group-shift method (sgs) introduced here better approximates the no-cutoff results than does group-based potential switching. Furthermore, the enhanced forces arising from the switched group-shift method do not worsen significantly as the switching region is narrowed (Fig. 1b, Table I), whereas those arising from group-based switching increase dramatically. Thus, switching from 11 to 12 Å produced inhibited fluctuation relative to the no-cutoff results with group-based switching but not with switched group-shifting (Table I).
4. When evaluating the realism embodied in a particular cutoff scheme, it is important to monitor the mean square fluctuation, $\langle(\underset{\sim}{\Delta r})^2\rangle$,

as well as the rmsd from the crystalline conformation or from the $t = 0$ structure. Atom- and group-based switching of the potential can produce seemingly desirable small conformational deviations by trapping the structure in artificial minima that inhibit motion severely.

5. Future biomolecular studies should reject simulations in vacuum with $\epsilon = r$ in favor of those using explicit or implicit solvation with a constant dielectric coefficient. Even when used with explicit solvent, the distance-dependent dielectric suppresses protein motion at high temperatures (Fig. 6).
6. Similarly, the shifted potential should not be used in future simulations. Figures 1, 3, and 4, Table I, and previous studies of liquid water have shown it to be inferior to the force-shifted potential in attenuating constant-dielectric electrostatic interactions. Because the force is first enhanced before it is reduced, it must be turned off rather abruptly at long distance (Fig. 1c), resulting in unnecessarily deep minima in the interaction energy of neutral groups (Fig. 4). We have used the shifted potential with $\epsilon = 1$ and $r_{off} = 12$ Å in our studies of the environmental dependence of MbCO dynamics.[10,30,33] With this cutoff distance, differences between it and better cutoff methods are not significant for MbCO. Nevertheless, we will discontinue use of the shifted potential.
7. Force shifting and force switching (with a 4-Å switching region) are the best atom-based cutoff methods. For these and the other energy-conserving methods, results improve as the cutoff is increased. That is, the rmsd from the X-ray conformation was better at $r_{off} = 15$ Å than it was at $r_{off} = 12$ Å, where it was better than at $r_{off} = 7.5$ Å. Although $\langle(\Delta r)^2\rangle$suffers from considerable statistical uncertainty, it also improved for force switching. These results are to be contrasted with the anomalous dependence of alpha helix stability on cutoff distance reported for simulations using group-based truncation.[7] We expect that our results are characteristic of energy-conserving spherical-cutoff methods that do not introduce artificial minima.
8. Simple test systems involving a few atoms, as in Figure 2, are extremely useful for evaluating modifications to the potential energy function. They provide the computational equivalent of a "back of the envelope" check that may reveal unforeseen consequences of the proposed modifications.

PROPOSED CRITERIA FOR LONG-RANGE FORCE MODIFICATIONS

Many spherical-cutoff methods have been analyzed here. To assess the physical realism embodied in any method of long-range potential modification, we propose, in order of importance, the following criteria:

1. No large forces are introduced at long range. Atom-based potential switching and group-based potential switching (in the presence of charged groups) fail this test miserably.
2. No deep energy minima are introduced into interactions between neutral groups. Deep energy minima arise whenever the force is trimmed too abruptly, as in force truncation and even in force switching from 11 to 12 Å (Fig. 3b). Relatively shallow minima arise in several of the methods tuned for short-range interactions (e.g., fsh4). These artificial energy minima inhibit molecular motion during MD simulation and are overpopulated in MC simulation.
3. Energy is conserved acceptably as the time step is reduced to zero. Group truncation applied to interactions involving polar groups results in continual heating as dipoles rotate near the cutoff. Strong coupling to a heat bath to draw energy from the system only masks the symptoms without curing the unphysical dynamics. Monotonic switching of group–group forces also fails to conserve energy regardless of the time step. However, our improved group-based method (sgs) does conserve energy and imposes a much smaller unphysical force (for charged groups) in the switching region than does traditional group-based switching (gsw).
4. Short-range forces are altered minimally. Cutoff methods that alter short-range forces may necessitate reparameterization of hydrogen bonding and other short-range interactions. Energetic parameters should not depend significantly on the cutoff distance.
5. The potential energy is a continuous function of the separation distance. Although energy

TABLE II.
Assessment of Methods with r_{off} = 12 Å in Terms of Proposed Criteria.

Cutoff method			Criterion 1	2	3	4	5	6	
Switch	(sw)	1 Å	x x x	x x x					(sw)
		4	x x	x x x					
Group-based truncation	(gtr)				x x x		x		(gtr)
Truncation	(tr)			x x x	x		x		(tr)
Force truncation	(ftr)			x x	x			*	(ftr)
Shift	(sh)			x		x x		x	(sh)
Eq. (15), β = 0	(fsh0)					x x x		x x	(fsh0)
Force shift; Eq. (15), β = 1	(fsh)					x		*	(fsh)
Eq. (15), β = 4	(fsh4)			x				*	(fsh4)
Group switch	(gsw)	1 Å	* * *						(gsw)
		4	* *						
Switched group-shift	(sgs)	1	*					*	(sgs)
		4	*					*	
Force switch	(fsw)	1		x x				*	(fsw)
		4		x				*	

Switching regions with widths of 1 and 4 Å are considered. Abbreviations are as in Figures 1 and 3. An 'x' indicates violation of the rule. An asterisk, '*' indicates violation only when charged groups are considered. Multiple x's or *'s reflect a pronounced negative side effect.

continuity has no effect on the evolution of an MD trajectory, it is important for MC simulation, energy minimization, and free-energy techniques that evaluate the relative energy of different conformations.

6. Group–group interaction energies are affected minimally at short range. The magnitude of group–group interactions should be preserved whenever this is consistent with criteria 1 through 5.

Table II compares the various potential modification schemes in light of our suggested criteria. It summarizes qualitatively the information plotted in the figures and tabulated in Table I. Simply put, comparing the method amounts to weighing the importance of preserving short-range forces against the need to trim forces gradually.

We propose that atom-based switching should never be used in any MD or MC simulation because both the interaction energy and force oscillate wildly as electrostatic interactions are turned on and off. Similarly, group–group switching should not be used in the presence of charged groups without the simple modification introduced here [eq. (14)]. The shifted potential is inferior to the force-shifted potential, but the differences in MbCO behavior simulated with these methods are slight with $r_{off} \geq 12$ Å.

Conclusions

As mentioned in the Introduction, mutagenesis experiments[1] lend support to the notion that interatomic forces can be turned off at long range to make large simulations computationally feasible without significantly destabilizing the macromolecule. Further evidence has been provided here: Even though the best atom-based methods (fsw, fsh, fsh4, fsh0, sh) appear to be very different in Figure 1c, they yield similar MbCO dynamics with r_{off} = 12 Å. That is, as long as gross errors are not introduced in the treatment of electrostatics (e.g., by switching the potential or by using too short a cutoff), attenuation of electrostatic forces by a spherical cutoff does not destabilize myoglobin or model hydrogen-bonding systems (Fig. 4). The differences in electrostatic forces as computed by the best cutoff methods with r_{off} = 12 Å are small in comparison to other forces (e.g., bond-stretching,

angle-bending, and torsional forces) resulting from the potential energy function.

This article identifies two superior atom-based spherical-cutoff methods and an improved group-based method: force switching, force shifting, and switched group-shifting. Choosing the appropriate method should be based on the charge character of the system of interest, the temperature to be simulated, and the hardware to be used. Our improved method of evaluating group–group interactions [sgs, eq. (14)] may be incorporated readily into existing programs tailored to a group–group framework. When the physical system of interest is composed solely of neutral groups (e.g., a pure water simulation), both switched group-shifting and atom-based force shifting give good results. Use of a vector machine may favor atom-based force shifting in this case. In principle (Fig. 1b) and in practice (Table I), atom-based force switching from 8 to 12 Å or from 11 to 15 Å becomes preferable to the other two methods in the presence of a significant number of charged groups. If low temperatures are to be simulated, the force-switching region should be wide enough and the cutoff long enough to avoid artificial minima with depths comparable to thermal energy.

Acknowledgments

We thank David C. Chatfield and Richard W. Pastor for valuable comments, Milan Hodošček for assistance with his parallelized version of CHARMM, and Stan Erwin and Robert Martino for support with the Intel iPSC/860 hypercube. P.J.S. thanks the National Research Council for a postdoctoral research associateship.

References

1. S. Dao-pin, E. Söderlind, W. A. Baase, J. A. Wozniak, U. Sauer, and B. W. Matthews, *J. Mol. Biol.*, **221,** 873 (1991).
2. C. L. Brooks III, B. M. Pettitt, and M. Karplus, *J. Chem. Phys.*, **83,** 5897 (1985).
3. C. L. Brooks III, *J. Phys. Chem.*, **90,** 6680 (1986).
4. C. L. Brooks III, *J. Chem. Phys.*, **86,** 5156 (1987).
5. R. J. Loncharich and B. R. Brooks, *Proteins*, **6,** 32 (1989).
6. D. B. Kitchen, F. Hirata, J. D. Westbrook, R. Levy, D. Kofke, and M. Yarmush, *J. Comp. Chem.*, **11,** 1169 (1990).
7. H. Schreiber and O. Steinhauser, *Biochemistry*, **31,** 5856 (1992).
8. K. Tasaki, S. McDonald, and J. W. Brady, *J. Comp. Chem.*, **14,** 278 (1993).
9. J. Guenot and P. A. Kollman, *J. Comp. Chem.*, **14,** 295 (1993).
10. P. J. Steinbach and B. R. Brooks, *Proc. Natl. Acad. Sci. USA*, **90,** 9135 (1993).
11. J. A. Board, Jr., J. W. Causey, J. F. Leathrum, Jr., A. Windemuth, and K. Schulten, *Chem. Phys. Lett.*, **198,** 89 (1992).
12. B. R. Brooks, R. E. Bruccoleri, B. D. Olafson, D. J. States, S. Swaminathan, and M. Karplus, *J. Comp. Chem.*, **4,** 187 (1983).
13. Polygen Corporation Parameter file for CHARMm version 20, Copyright 1986, released August 1988.
14. J. D. Madura and B. M. Pettitt, *Chem. Phys. Lett.*, **150,** 105 (1988).
15. A. Rahman and F. H. Stillinger, *J. Chem. Phys.*, **55,** 3336 (1971).
16. D. J. Adams, E. M. Adams, and G. J. Hills, *Mol. Phys.*, **38,** 387 (1979).
17. H. J. C. Berendsen, J. P. M. Postma, W. F. van Gunsteren, A. DiNola, and J. R. Haak, *J. Chem. Phys.*, **81,** 3684 (1984).
18. J. Pleiss and F. Jähnig, *Biophys. J.*, **59,** 795 (1991).
19. J. A. Rupley and G. Careri, *Adv. Prot. Chem.*, **41,** 37 (1991).
20. O. Teleman, *Mol. Simul.*, **1,** 345 (1988).
21. P. E. Smith and B. M. Pettitt, *J. Chem. Phys.*, **95,** 8430 (1991).
22. J. Smith, K. Kuczera, and M. Karplus, *Proc. Natl. Acad. Sci. USA*, **87,** 1601 (1990).
23. K. Kuczera, J. Kuriyan, and M. Karplus, J. Mol. Biol., **213,** 351 (1990).
24. M. P. Allen and D. J. Tildesley, *Computer Simulation of Liquids*, Oxford University Press, Oxford 1987, and references therein.
25. M. Prevost, D. van Belle, G. Lippens, and S. Wodak, *Mol. Phys.*, **71,** 587 (1990).
26. M. E. Tuckerman, B. J. Berne, and G. J. Martyna, *J. Chem. Phys.*, **94,** 6811 (1991).
27. W. L. Jorgensen, J. Chandrasekhar, J. D. Madura, R. W. Impey, and M. L. Klein, *J. Chem. Phys.*, **79,** 926 (1983).
28. B. R. Brooks and M. Hodošček, *Chem. Des. Auto. News*, **7,** 16 (1992).
29. J. Kuriyan, S. Wilz, M. Karplus, and G. A. Petsko, *J. Mol. Biol.*, **192,** 133 (1986).
30. R. J. Loncharich and B. R. Brooks, *J. Mol. Biol.*, **215,** 439 (1990).
31. W. Doster, S. Cusack, and W. Petry, *Nature*, **337,** 754 (1989).
32. H.-Q. Ding, N. Karasawa, and W. A. Goddard III, *J. Chem. Phys.*, **97,** 4309 (1992).
33. P. J. Steinbach, R. J. Loncharich, and B. R. Brooks, *Chem. Phys.*, **158,** 383 (1991).